Bengt Hallstedt, Olga Kim*
Materials Chemistry, RWTH Aachen University, Aachen, Germany
*Now with Max-Planck-Institut für Eisenforschung, Düsseldorf, Germany

Thermodynamic assessment of the Al–Li system

Dedicated to Dr. Gunnar Eriksson on the occasion of his 65th birthday

In the present work a Calphad type thermodynamic assessment of the Al–Li system is presented. The system is dominated by the central AlLi phase, which has an ordered bcc (B32) structure. fcc Al dissolves considerable amounts of Li. If the fcc solid solution is quenched from high temperature, coherent metastable Al_3Li precipitates with an ordered fcc ($L1_2$) structure can form. There are two nearly stoichiometric phases; Al_2Li_3 and Al_4Li_9. The disordered fcc phase and the ordered Al_3Li phase as well as the disordered bcc phase (Li) and the ordered AlLi phase are described by four-sublattice models. There is a fairly complete set of experimental data available for this system, and most of them are satisfactorily described by the currently optimised parameters.

Keywords: Al–Li; Phase diagram; Calphad; Thermodynamics

1. Introduction

Al dissolves up to about 15 at.% Li, thereby decreasing density and increasing Young's modulus. Al–Li based alloys can also be precipitation hardened by metastable coherent Al_3Li precipitates with the $L1_2$ structure. In spite of the difficulties in handling Li, Al–Li based alloys have found some use as high strength, low density materials [1–3]. They are then typically alloyed with Mg and/or Cu. Two-phase mixtures of fcc-Al and AlLi (B32 structure) deliver a stable emf of about 300 mV relative to liquid Li, and played some role in the early development of Li batteries [4, 5].

The Al–Li system contains three stable intermediate phases; β (AlLi), Al_2Li_3 and Al_4Li_9 (see Fig. 1). There is also a metastable intermediate phase; α′ (Al_3Li). A list of the phases and their alternative names is given in Table 1. The phase diagram is dominated by the β phase, which shows a considerable homogeneity range and melts congruently around 970 K. fcc-Al (α) dissolves up to about 15 at.% Li at the eutectic temperature, decreasing with decreasing temperature. At low temperature, the metastable Li solubility in equilibrium with α′ is considerably higher than the equilibrium solubility. The phases Al_2Li_3 and Al_4Li_9 show narrow, but essentially unknown, homogeneity ranges. They are treated as stoichiometric in this work. Solid Li (bcc) dissolves a small, but unknown, amount of Al.

The Al–Li system has been partially or completely modelled thermodynamically a number of times [6–11]. The most complete, and probably most accurate, description to date is by Saunders [10]. McAlister [7] made an extensive review of the, then available, experimental data. In this work we make a Calphad type evaluation of the available experimental data, including data from ab-initio calculations of total energies of various ordered structures. For the fcc-based and bcc-based phases four-sublattice ordering models are used.

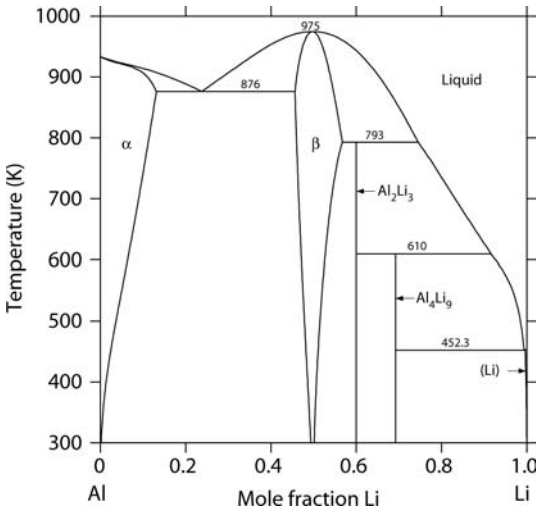

Fig. 1. The calculated Al–Li phase diagram.

Table 1. Phases in the Al–Li System.

Phase	Also known as	Prototype	Pearson symbol	Strukturbericht
α	fcc-Al	Cu	cF4	A1
α′	Al_3Li, δ′	$AuCu_3$	cP4	$L1_2$
β	AlLi, δ	NaTl	cF16	B32
Al_2Li_3	δ	Ga_2Te_3	hR15	–
Al_4Li_9	γ	Al_4Li_9	mC26	–
(Li)	bcc-Li	W	cI2	A2

2. Experimental data

2.1. Phase diagram data

There have been a number of early investigations of the Al–Li system [12–15]. The amount of impurities can be expected to have been high in these investigations. Grube et al. [14] quote an Fe-content of up to 0.75 at.% in their alloys. In spite of this, these early data are for most part in fairly good agreement with more recent data. The most ac-

curate and extensive appear to be those of Shamray and Saldau [15]. The currently accepted phase diagram, with the Al_2Li_3 and Al_4Li_9 phases, was essentially established by Myles et al. [16]. The crystal structure of Al_2Li_3 was determined by Tebbe et al. [17] and the crystal structure of Al_4Li_9 was determined by Hansen and Smith [18]. The most extensive and consistent investigation of the phase diagram has been made by Schürmann and Voss [19]. Unfortunately, they misinterpreted their results for high Li contents and assigned a high Al solubility in bcc-Li and did not identify the Al_4Li_9 phase. They also assigned the composition $AlLi_2$ to the Al_2Li_3 phase. When assigned to the correct equilibria, their liquidus data and invariant temperatures appear to be reasonable, though. There is a very good agreement among the sources on the invariant temperatures and a good agreement on the liquidus on the Al-rich side of the system, but a very large scatter on the liquidus on the Li-rich side. Recent data on the Li-rich liquidus from Pulham et al. [20] are in good agreement with the data from Schürmann and Voss [19]. The difference between the melting temperature of pure Li and the eutectic temperature is insignificant, suggesting that the Al solubility in bcc-Li is small. There is no direct measurement. There is a thermal event at 540 or 515 K [16, 19] suggesting a transition in the Al_4Li_9 phase. However, this was not seen by Pulham et al. [20] in their investigation.

There are a large number of investigations on the α solvus [14–16, 21–28]. The scatter is also large, particularly at low temperature. A few of the data points can be assigned to the metastable $\alpha + \alpha'$ equilibrium, rather than the stable $\alpha + \beta$ equilibrium. The data of Schürmann and Geißler [27] appear to be the most consistent and reliable. There have also been a number of investigations of the metastable $\alpha + \alpha'$ equilibrium [26, 29–33]. Here the most consistent data are those of Cocco et al. [31].

The β phase is stable approximately in the range $0.45 < x_{Li} < 0.56$. There is a large scatter among the experimental data [19, 25, 27, 34–37], both regarding the absolute values and their temperature dependence. The most reasonable and internally consistent data are those of Wen et al. [35] and those of Amezawa et al. [37], both using emf methods. The difference between the two sources is quite large, though, and no preference could be given to one or the other.

2.2. Thermodynamic data

There are no direct measurements of enthalpies of formation, but there are several ab initio total energy calculations at 0 K, both of the stable phases and of a number of ordered phases based on the bcc and fcc lattices [38–42]. These can be directly taken as enthalpies. The maximum difference among the stable phases is about 4 kJ mol^{-1}. According to Sluiter et al. [42] the structural energy differences from Guo et al. [39] can be assumed to be the more accurate. The enthalpy of formation at 298 K of the β phase evaluated from emf data on the $\alpha + \beta$ equilibrium was found to be −21.8 kJ mol^{-1} by Yao et al. [43], in perfect agreement with the ab-initio value from Guo et al. [39].

The enthalpy of mixing of the liquid has been measured by Bushmanov and Yatsenko [44] and Moser et al. [45] in good mutual agreement. The partial enthalpy has been measured by Lee and Sommer [46]. Li activities in the liquid have been measured by Hicter et al. [47] and Yatsenko and Saltykova [48], also in good mutual agreement.

There have been a number of emf measurements of Li potentials among the solid phases in the temperature range 550 to 875 K [28, 35, 37, 43, 49–51]. All measurements were made relative to pure liquid Li. Zaitsev et al. [52] used Knudsen Mass Spectrometry (KMS) to measure Li potentials in the α single phase region and in the $\alpha + \beta$ two-phase region. In addition Li potential measurements in the β single phase region were made by Veleckis [36] using a hydrogen titration method. The hydrogen pressure could then be converted to Li potential. The emf of the $\alpha + \beta$ equilibrium is excellently reproducible and the equation given by Wen et al. [35] ($E = 451 - 0.220T$ mV) was accepted. All other measurements, in particular in the α and β single phase regions, showed smaller or larger systematic contradictions. The measurements of Zaitsev et al. [52] in the α single phase region are excellently consistent with the $\alpha + \beta$ measurements, which is not the case with the emf measurements from Wen et al. [35].

3. Thermodynamic models

3.1. Elements, liquid and stoichiometric phases

The descriptions of pure bcc, fcc and liquid Al and Li are taken from Dinsdale [53]. The composition dependence of the liquid phase is described using standard Redlich–Kister polynomials [54, 55] with a linear temperature dependence. The two phases Al_2Li_3 and Al_4Li_9 are described as stoichiometric phases and their Gibbs energies are expressed relative to fcc-Al and bcc-Li:

$$G^{\phi}_{Al_iLi_j} = i\,{}^{o}G^{fcc}_{Al} + j\,{}^{o}G^{bcc}_{Li} + A^{\phi} + B^{\phi}T \quad (1)$$

3.2. fcc-based ordering

The fcc phase is described by four sublattices using a Bragg–Williams–Gorsky [56, 57] based model essentially following the approach described by Kusoffsky et al. [58]. The four sublattices are identical and the model, thus, symmetrical. It is used to describe the ordered $L1_0$ (AlLi) and $L1_2$ (Al_3Li and $AlLi_3$) and disordered fcc phases. The Gibbs energy is split into an order independent contribution and an order dependent contribution:

$$G^{fcc} = G^{dis}(x_i) + \Delta G^{ord}(y^s_i) \quad (2)$$

When the phase is disordered, the ordering energy is zero. This is given by expressing the ordering energy as:

$$\Delta G^{ord} = G^{4sl}(y^s_i) - G^{4sl}(y^s_i = x_i) \quad (3)$$

The Gibbs energies of the ordered compounds are described in the following manner:

$$G^{4sl}_{Al:Al:Al:Li} = G^{4sl}_{Al:Al:Li:Al} = ... = G^{4sl}_{Al_3Li} = 3u + \Delta G_{Al_3Li} \quad (4)$$

$$G^{4sl}_{Al:Al:Li:Li} = G^{4sl}_{Al:Li:Al:Li} = ... = G^{4sl}_{Al_2Li_2} = 4u \quad (5)$$

$$G^{4sl}_{Al:Li:Li:Li} = G^{4sl}_{Li:Al:Li:Li} = ... = G^{4sl}_{AlLi_3} = 3u + \Delta G_{AlLi_3} \quad (6)$$

All Gibbs energies are given for one mole of atoms. Interactions are assumed to be independent on which sublattice they take place (required by symmetry) and the occupation of the other sublattices:

$$L^{4sl}_{Al,Li:*:*:*} = L^{4sl}_{*:Al,Li:*:*} = ... = L^{4sl} \quad (7)$$

In addition a reciprocal interaction is introduced to simulate short range order:

$$L^{4sl}_{Al,Li:Al,Li:*:*} = L^{4sl}_{Al,Li:*:Al,Li:*} = ... = L^{4sl}_{rec} = u \quad (8)$$

In principle, the reciprocal interaction can be optimised, but this did not bring any improvement for the fcc phase. The interaction parameters for the disordered phase were related to the ordering parameters in the following manner:

$${}^0L^{dis}_{Al,Li} = G^{4sl}_{Al_3Li} + 1.5G^{4sl}_{Al_2Li_2} + G^{4sl}_{AlLi_3} + 1.5L^{4sl}_{rec} + 4\,{}^0L^{4sl} \quad (9)$$

$${}^1L^{dis}_{Al,Li} = 2G^{4sl}_{Al_3Li} - 2G^{4sl}_{AlLi_3} + 4\,{}^1L^{4sl} \quad (10)$$

$${}^2L^{dis}_{Al,Li} = G^{4sl}_{Al_3Li} - 1.5G^{4sl}_{Al_2Li_2} + G^{4sl}_{AlLi_3} - 1.5L^{4sl}_{rec} + 4\,{}^2L^{4sl} \quad (11)$$

3.3. bcc-based ordering

The bcc phase is also described using a four-sublattice model. This model can describe the ordered B2 (AlLi), B32 (AlLi) and $D0_3$ (Al_3Li and $AlLi_3$) and disordered bcc phases. Actually, the $D0_3$ phase is considerably more complex than the corresponding fcc phase ($L1_2$) [59]. In the $D0_3$ phase only two sublattices need to be identically occupied in contrast to $L1_2$ where three sublattices are identically occupied. When two nearest neighbour sublattices are identical the order is $F\bar{4}3m$ and when two next nearest neighbour sublattices are identical the order is $D0_3$ ($Fm3m$) [59]. At least in this system it turned out that the energy differences between these two possibilities are very small. At the perfectly ordered ground state at 0 K there is no difference between these two ordering possibilities. In the following no distinction will be made between $F\bar{4}3m$ and $D0_3$.

Kishio and Brittain [34] showed that vacancies dominate as defects on the lithium sublattices and lithium anti-structure atoms dominate on the aluminium sublattices. Although, a treatment of the bcc phase including vacancies would be desirable we decided against it. A four-sublattice treatment including vacancies would increase the complexity to such an extent that it can only be handled with difficulty, at least at this stage. The number of compound energies would increase from 16 to 81. Furthermore, the compound energies concerning the B2 and $D0_3$ phases are not experimentally accessible, but have to be determined using ab-initio data (or estimations) and all ab-initio data currently available concern perfectly ordered compounds without vacancies.

In contrast to the fcc phase the sublattices are not identical any more [60]. It is assumed here that atoms on the first sublattice has nearest neighbours on the third and fourth sublattices and next nearest neighbours on the second sublattice. This leads to the following Gibbs energies for the ordered compounds:

$$G^{4sl}_{Al:Al:Al:Li} = G^{4sl}_{Al:Al:Li:Al} = ... = G^{4sl}_{Al_3Li} = 2u_1 + 1.5u_2 + \Delta G_{Al_3Li} \quad (12)$$

$$G^{4sl}_{Al:Al:Li:Li} = G^{4sl}_{Li:Li:Al:Al} = G^{B2}_{Al_2Li_2} = 4u_1 \quad (B2) \quad (13)$$

$$G^{4sl}_{Al:Li:Al:Li} = G^{4sl}_{Al:Li:Li:Al} = ... = G^{B32}_{Al_2Li_2} = 2u_1 + 3u_2 \quad (B32) \quad (14)$$

$$G^{4sl}_{Al:Li:Li:Li} = G^{4sl}_{Li:Al:Li:Li} = ... = G^{4sl}_{AlLi_3} = 2u_1 + 1.5u_2 + \Delta G_{AlLi_3} \quad (15)$$

Here u_1 is essentially the bond exchange energy between nearest neighbours and u_2 is the bond exchange energy between next nearest neighbours. Interactions can be added as for the fcc phase, but they turned out not to be necessary in this case. Short range order is assumed to be less important for the bcc phase than for the fcc phase, but it turned out to be very useful to include a reciprocal interaction. For the bcc phase two different reciprocal interactions are possible, but they are set equal here. In contrast to the fcc phase, the reciprocal interaction was independently optimised and not included in the expressions for the interaction parameters for the disordered phase. Otherwise it was not possible to reproduce the width of the β phase field. The interaction parameters for the disordered phase were related to the ordering parameters in the following manner:

$${}^0L^{dis}_{Al,Li} = G^{4sl}_{Al_3Li} + 0.5G^{B2}_{Al_2Li_2} + G^{B32}_{Al_2Li_2} + G^{4sl}_{AlLi_3} + 4\,{}^0L^{4sl} \quad (16)$$

$${}^1L^{dis}_{Al,Li} = 2G^{4sl}_{Al_3Li} - 2G^{4sl}_{AlLi_3} + 4\,{}^1L^{4sl} \quad (17)$$

$${}^2L^{dis}_{Al,Li} = G^{4sl}_{Al_3Li} - 0.5G^{B2}_{Al_2Li_2} - G^{B32}_{Al_2Li_2} + G^{4sl}_{AlLi_3} + 4\,{}^2L^{4sl} \quad (18)$$

4. Optimisation of parameters

The optimisation was performed using the Parrot module of the Thermo-Calc software package [61]. All calculations were made using the Thermo-Calc package. Start values for the parameters were taken from the work of Saunders [10], except for the β phase. All ordering parameters were preliminarily fixed according to the ab-initio formation energies from Guo et al. [39], with the exception of a temperature dependent parameter for the β (B32) phase. Start values for the β phase had to be found be trial and error. It turned out to be necessary to use a reciprocal interaction for the β (ordered bcc) phase, otherwise the β phase field remained very narrow. All parameters for the stable phases were then optimised and the weights of the experimental data adjusted until a reasonable result was found. It was also tested if some parameters could be removed. For the α phase it was enough to use a temperature-dependent regular interaction. The major part of the interaction was taken care of by the ordering parameters. For the liquid it was necessary to use a rather large number of parameters. An attempt to remove the highest order (${}^3L$ and/or ${}^4L$) interac-

tions led to a significant increase in the error sum. Finally, the ordering parameters were included in the optimisation and the ab-initio data from Guo et al. [39] and the $\alpha + \alpha'$ data from Cocco et al. [31] added to the experimental data set. It was not possible to optimise the ordering parameters related to the Al_3Li ($D0_3$) and $AlLi_3$ ($L1_2$) phases. The inclusion of the fcc ordering parameters and $\alpha + \alpha'$ data led to a shift of the stable α solvus towards higher Li content. This could be counteracted to some extent by increasing the weight on the α solvus data. The $D0_3$ ordering parameters turned out to have a rather strong influence on the shape and symmetry of the β phase field.

The following experimental data were used in the optimisation. Invariant temperatures from Schürmann and Voss [19] and Myles et al. [16] were used with a high weight, and the corresponding compositions with a lower weight. Liquidus data from Schürmann and Voss [19] and Pulham et al. [20] were used. Solidus data on the α phase [10] were used with a relatively low weight. Solvus data of the α phase [15, 24, 27, 28] were used with equal weights. Data on the β phase boundaries were taken from the emf based data from Wen et al. [35] and Amezawa et al. [37]. They were given equal weights. Enthalpies of mixing in the liquid [44, 45], enthalpy of melting of β [44] and Li activities in the liquid [47, 48] were included. Emf data on the $\alpha + \beta$ equilibrium [35, 43, 51] and KMS data on Li potentials in the α phase [52] were used with high weight. Emf data on Li potentials in the β phase [35, 37] were used with low weight.

Table 2. Thermodynamic parameters for the Al–Li system determined in the present work.

Liquid

$$L = -44\,200 + 20.6T + (13\,600 - 5.3T)(x_{Al} - x_{Li}) + 14\,200(x_{Al} - x_{Li})^2$$
$$-12\,100(x_{Al} - x_{Li})^3 - 7100(x_{Al} - x_{Li})^4$$

fcc(A1, $L1_0$, $L1_2$)

$$^0L^{dis}_{Al,Li} = G^{4sl}_{Al_3Li} + 1.5G^{4sl}_{Al_2Li_2} + G^{4sl}_{AlLi_3} + 1.5L^{4sl}_{rec} + 4\,^0L^{4sl}$$
$$^1L^{dis}_{Al,Li} = 2G^{4sl}_{Al_3Li} - 2G^{4sl}_{AlLi_3} + 4\,^1L^{4sl}$$
$$^2L^{dis}_{Al,Li} = G^{4sl}_{Al_3Li} - 1.5G^{4sl}_{Al_2Li_2} + G^{4sl}_{AlLi_3} - 1.5L^{4sl}_{rec} + 4\,^2L^{4sl}$$
$$^0L^{4sl} = 2960 - 1.56T, {}^1L^{4sl} = {}^2L^{4sl} = 0$$
$$G^{4sl}_{Al_3Li} = 3u + \Delta G_{Al_3Li}$$
$$G^{4sl}_{Al_2Li_2} = 4u$$
$$G^{4sl}_{AlLi_3} = 3u + \Delta G_{AlLi_3}$$
$$L^{4sl}_{rec} = u$$
$$u = -3270 + 1.96T$$
$$\Delta G_{Al_3Li} = 1750 - 4.7T$$
$$\Delta G_{AlLi_3} = 4900$$

bcc(A2, B2, B32, $D0_3$)

$$^0L^{dis}_{Al,Li} = G^{4sl}_{Al_3Li} + 0.5G^{B2}_{Al_2Li_2} + G^{B32}_{Al_2Li_2} + G^{4sl}_{AlLi_3} + 4\,^0L^{4sl}$$
$$^1L^{dis}_{Al,Li} = 2G^{4sl}_{Al_3Li} - 2G^{4sl}_{AlLi_3} + 4\,^1L^{4sl}$$
$$^2L^{dis}_{Al,Li} = G^{4sl}_{Al_3Li} - 0.5G^{B2}_{Al_2Li_2} - G^{B32}_{Al_2Li_2} + G^{4sl}_{AlLi_3} + 4\,^2L^{4sl}$$
$$^0L^{4sl} = {}^1L^{4sl} = {}^2L^{4sl} = 0$$
$$G^{4sl}_{Al_3Li} = 2u_1 + 1.5u_2 + \Delta G_{Al_3Li}$$
$$G^{B2}_{Al_2Li_2} = 4u_1 \quad (B2)$$
$$G^{B32}_{Al_2Li_2} = 2u_1 + 3u_2 \quad (B32)$$
$$G^{4sl}_{AlLi_3} = 2u_1 + 1.5u_2 + \Delta G_{AlLi_3}$$
$$L^{4sl}_{rec} = 15\,000$$
$$u_1 = -3360 + 1.8T$$
$$u_2 = -4230 + 1.86T$$
$$\Delta G_{Al_3Li} = 3700$$
$$\Delta G_{AlLi_3} = 3250$$

Al_2Li_3

$$G^{Al_2Li_3} = 2\,^oG^{fcc}_{Al} + 3\,^oG^{bcc}_{Li} - 93\,990 + 34.5T$$

Al_4Li_9

$$G^{Al_4Li_9} = 4\,^oG^{fcc}_{Al} + 9\,^oG^{bcc}_{Li} - 193\,780 + 71.7T$$

All parameter values are given in SI units (J, mol, K; $R = 8.31447$ J mol^{-1} K^{-1}).

Table 3. Invariant Equilibria in the Al–Li System.

Reaction on cooling	Temperature (K)	Compositions, x_{Li}			Reference
$L \rightarrow \beta$	991	–	–	–	[15]
	965	–	–	–	[16]
	970	0.49	0.49	–	[19]
	975	0.497	0.497	–	This work
$L \rightarrow \alpha + \beta$	871	0.247	0.124	–	[12]
	863	0.234	0.124	–	[13]
	873	0.30	0.18	–	[14]
	871	0.26	–	–	[15]
	873	–	–	–	[16]
	875	0.252	0.138	0.475	[19]
	873	0.258	–	–	[9]
	876	0.238	0.131	0.456	This work
$\beta + L \rightarrow Al_2Li_3$	794	0.56	0.78	0.667	[14]
	793	–	0.70	–	[15]
	793	–	–	0.600	[16]
	792	0.58	0.756	0.667	[19]
	793	0.567	0.745	0.600	This work
$Al_2Li_3 + L \rightarrow Al_4Li_9$	608	0.600	–	0.692	[16]
	620	0.600	0.908	0.692	[20]
	610	0.600	0.916	0.692	This work
$L \rightarrow Al_4Li_9 + (Li)$	453	–	0.692	–	[16]
	453.6	0.994	0.692	–	[20]
	452.3	0.9932	0.692	0.9957	This work

5. Results and discussion

The optimised set of parameters is given in Table 2 and the calculated (stable) phase diagram is shown in Fig. 1. Calculated and experimental data on invariant equilibria are given in Table 3. The calculated temperatures are all very close to the experimental ones. Both the calculated α and liquid compositions at the α + β eutectic are slightly low. For the β phase, composition data are inconclusive. The calculated Al solubility in solid Li is slightly lower than in the liquid at the eutectic. This was achieved without adding any particular constraints for solid Li (bcc), except experimental data on the liquid composition and the eutectic temperature.

The liquidus and solidus of the α phase are shown in Fig. 2 together with experimental data. The liquidus data are described very well. The data on the α solidus are inconclusive. At higher Li content the calculation agrees fairly well with the data of Schürmann and Voss [19]. The α + Liquid two-phase region is very narrow for low Li contents. This was not possible to change without losing the good fit of the liquidus data. If the weight on the liquidus data was reduced there was a tendency to form a maximum close to pure Al, leading to much higher liquidus temperatures. The β liquidus is shown in Fig. 3. The calculation is very close to the data of Schürmann and Voss [19]. On the Li-rich side the scatter among the experimental data is very large. The data of Myles et al. [16] are fairly close to those of Schürmann and Voss [19], whereas Grube et al. [14] show too high temperatures and Shamray and Saldau [15] show too low temperatures. The Li-rich liquidus is shown

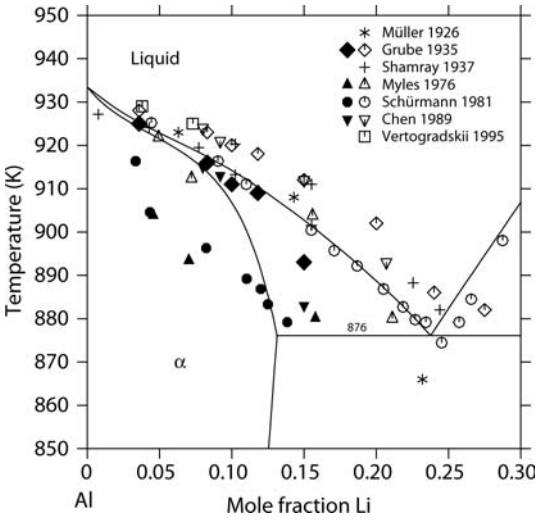

Fig. 2. Calculated α liquidus and solidus including experimental data [9, 13–16, 19, 62].

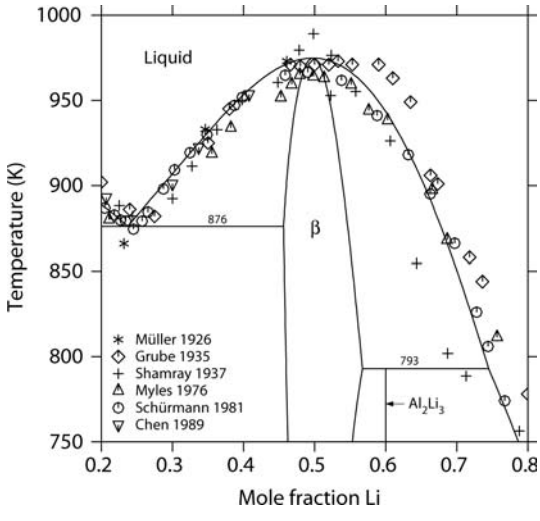

Fig. 3. Calculated β liquidus and solidus including experimental data on the β liquidus [9,13–16, 19].

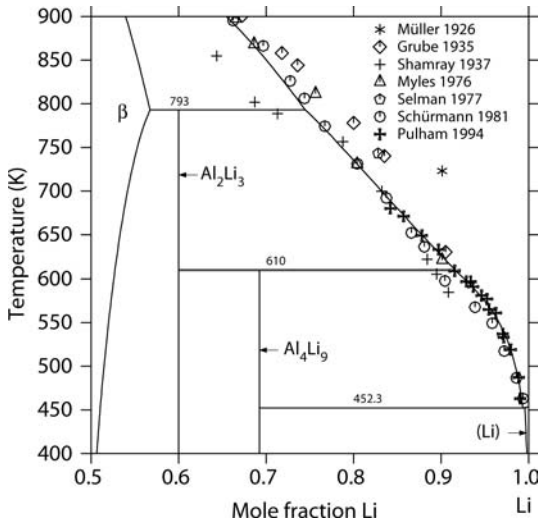

Fig. 4. Calculated liquidus of the Li-rich part of the Al–Li system including experimental data [13–16, 19, 20, 50].

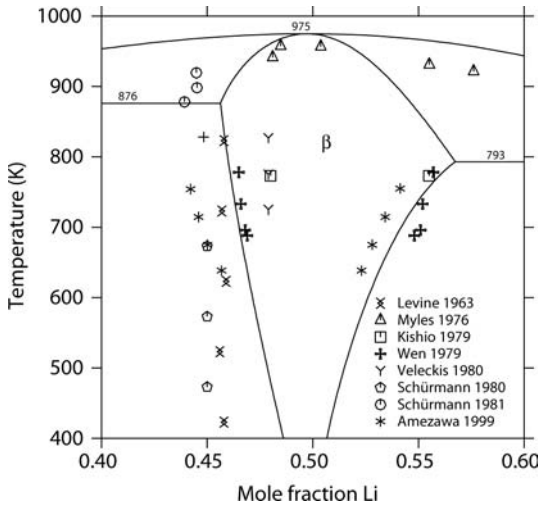

Fig. 5. Calculated β phase field including experimental data on the β phase boundaries [16, 19, 25, 27, 34–37].

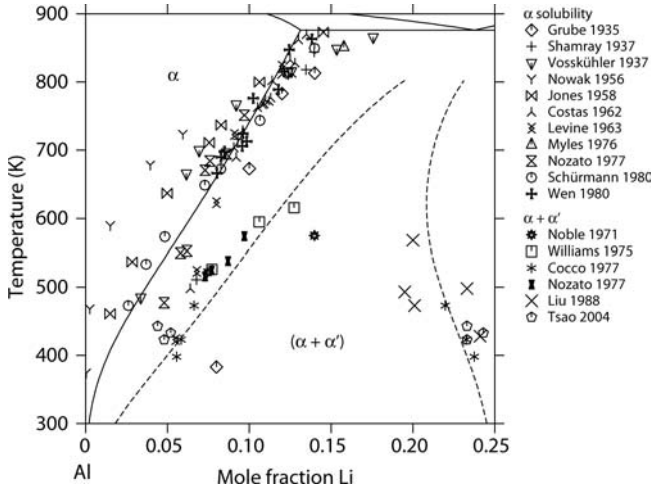

Fig. 6. Calculated solvus of the α phase and metastable α/α′ phase boundaries (dashed) including experimental data [14–16, 21–33].

in Fig. 4. The calculated liquidus is close to the data of both Schürmann and Voss [19] and Pulham et al. [20].

The single phase region of the β phase is shown in Fig. 5. As mentioned earlier the experimental data from Wen et al. [35] and Amezawa et al. [37] were used with equal weight. No other data were used. The optimisation itself did not reveal a clear preference towards one dataset. The Li-rich phase boundary shows a slightly stronger increase in Li content than suggested by the experimental data. This "asymmetry" is connected with the relatively high stability of the $AlLi_3$ ($D0_3$) phase compared to the Al_3Li ($D0_3$) phase. It was actually possible to "adjust" the positions of the β phase boundaries to some extent by changing the energies of the $AlLi_3$ ($D0_3$) and Al_3Li ($D0_3$) compounds.

The Li solubility in the α phase (α solvus) is shown in Figs. 6 and 7. In addition the metastable $\alpha + \alpha'$ phase boundaries are shown in Fig. 6. There is a very large scatter

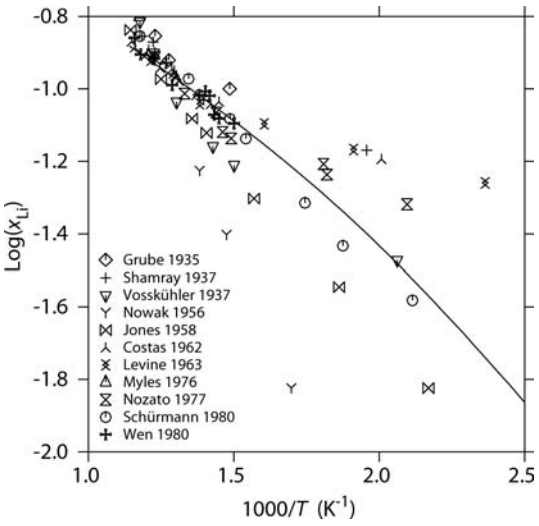

Fig. 7. Calculated solvus of the α phase including experimental data [14–16, 21–28].

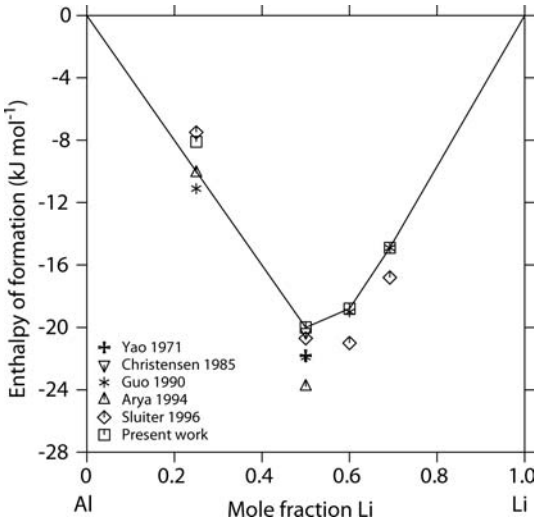

Fig. 8. Enthalpies of formation of the stable phases and α′ from the present calculation, ab-initio calculations [38–40, 42] and experimental data [43]. The present calculation and the experimental data refer to 298.15 K and the ab-initio data refer to 0 K. All data are for one mole of atoms relative to fcc-Al and bcc-Li. The lines simply connect the calculated values for the stable phases to guide the eye.

among the data, in particular at low temperature. It is clear that some of the low temperature data, believed by the original authors to belong to the stable α solvus, actually belong to the metastable α solvus. In this work the data of Schürmann and Geißler [27] were assumed to be the most accurate. There are no really solid arguments to substantiate this assumption, except that their data lie on a reasonable line when extrapolating the majority of the high temperature data (see Fig. 7). The calculated line appears to be somewhat more straight than suggested by the experimental data in Fig. 6 and the solubility is somewhat low at higher temperatures. The metastable $\alpha + \alpha'$ equilibrium is very well reproduced, although the scatter among the experimental data is very large.

Calculated enthalpies of formation are compared with ab-initio energies in Fig. 8 for the stable phases (and α') and in Table 4 for the stable phases and the possible fcc- and bcc-based ordered structures. In most cases there is a good agreement with the data of Guo et al. [39]. The exception is the Al_3Li ($D0_3$) phase, which according to Guo et al. [39] should be considerably less stable. The present value is closer to those of Das et al. [41] and Sluiter et al. [42]. Decreasing the stability compared to the $AlLi_3$ ($D0_3$) phase led to unwanted changes in the phase boundaries of the β phase.

Table 4. Enthalpies of formation of ordered phases in the Al–Li System. The reference states are fcc-Al and bcc-Li.

Phase	ΔH (kJ/(mol atoms))	Reference
Al_3Li ($L1_2$)	−11.1	[39]
	−10.1	[40]
	−7.5	[42]
	−8.1	This work
AlLi (B32)	−21.8	[43]
	−20.3	[38]
	−21.9	[39]
	−23.8	[40]
	−20.7	[42]
	−20.0	This work
Al_2Li_3	−19.0	[39]
	−21.0	[42]
	−18.8	This work
Al_4Li_9	−14.9	[39]
	−16.8	[42]
	−14.9	This work
Al_3Li ($D0_3$)	+1.9	[39]
	−4.8	[41]
	−3.9	[42]
	−5.0	This work
AlLi (B2)	+6.1	[38]
	−13.7	[39]
	−16.4	[41]
	−13.8	[42]
	−14.0	This work
AlLi ($L1_0$)	−13.7	[39]
	−11.9	[40]
	−9.5	[42]
	−13.1	This work
$AlLi_3$ ($D0_3$)	−10.9	[39]
	−12.0	[41]
	−10.2	[42]
	−10.5	This work
$AlLi_3$ ($L1_2$)	−6.5	[39]
	−5.0	[40]
	−2.3	[42]
	−5.0	This work

The enthalpy of mixing in the liquid phase is shown in Fig. 9. The agreement with experimental data is good. There is no temperature dependence of the calculated enthalpy of mixing. The calculated enthalpy of melting of the β phase is 14.8 kJ mol^{-1} compared to 16.7 kJ mol^{-1} measured by Bushmanov and Yatsenko [44]. The partial enthalpy of mixing of Li at low Li content at 1200 K was calculated to be −35.5 kJ mol^{-1} compared to the experimental value of −22.6 kJ mol^{-1} [46]. Li activities in the liquid at 987 K are shown in Fig. 10. The calculated activities are somewhat lower than the experimental data for $x_{Li} > 0.2$. Data at 957 K [47] and 1023 K [48] compare similarly. Even when increasing the weight of these data, the fit did not improve significantly. The reason is certainly not a lack of variable coefficients for the liquid interaction, but probably an incompatibility with data involving the β phase.

The Al–Li potential diagram is shown in Fig. 11 with the Li potential expressed as emf relative to pure liquid Li. Ex-

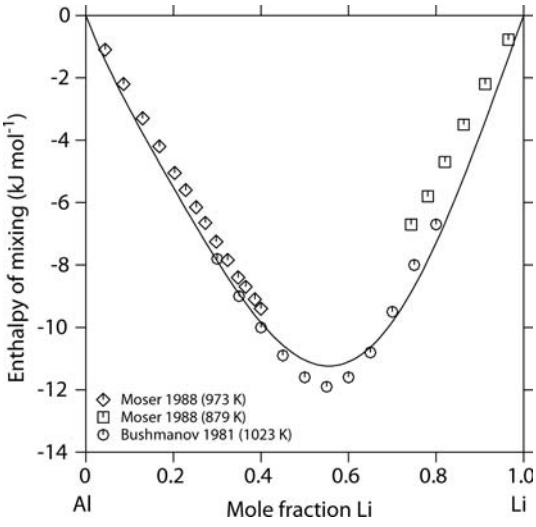

Fig. 9. Calculated enthalpy of mixing in the liquid phase including experimental data [44, 45].

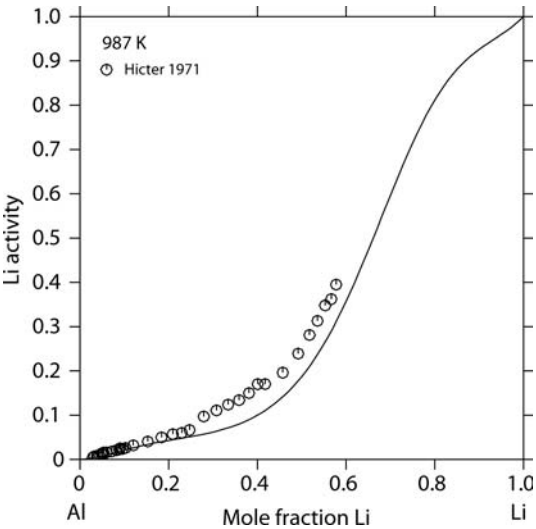

Fig. 10. Calculated Li activity in the liquid phase at 987 K including experimental data [47].

perimental data on the $\alpha + \beta$ equilibrium are fitted perfectly. They were also given a high weight during the optimisation. Data on the $\beta + Al_2Li_3$ and Al_2Li_3 + liquid equilibria from Amezawa et al. [37] are also reproduced well, although they were given only a low weight during the optimisation. Data from Selman et al. [50] and Wen et al. [35] on the $\beta + Al_2Li_3$ equilibrium are completely incompatible with other data. Li potentials for a number of compositions in the α phase are shown in Fig. 12. The fit to the data from Zaitsev et al. [52] is very good. The Li potentials measured by Wen et al. [35] are obviously much too low. Li potentials across the whole system at 696 K are shown in Fig. 13. The agreement with experimental data is generally good except with the data from Wen et al. [35] in the α single phase region. It is possible that there is a general problem with emf measurements in the α single phase region. When looking more in detail on the β phase region some discrepancies are revealed (Fig. 14). Whereas the general agreement is fairly good, there are large differences in detail, in particular the shape of the curves. Possibly, the shape of the curves could be changed by including vacancies in the bcc ordering model. An optimisation could be difficult, though, since the experimental data may have to be shifted in composition somewhat before it can be used. The difference between the two datasets shown in Fig. 14 is much larger (and in the opposite direction) than could be explained by the difference in temperature. Further measurements at 639, 675 and 754 K [37] and 688 and 778 K [35] compare similarly. The hydrogen titration data across the β phase from Veleckis [36] are reasonably well reproduced, but with some differences in detail.

6. Conclusion

Most of the experimental data on the Al–Li system are well described by the present thermodynamic description. There are some minor differences which have been discussed in the text. Considering the fairly complete set of experimen-

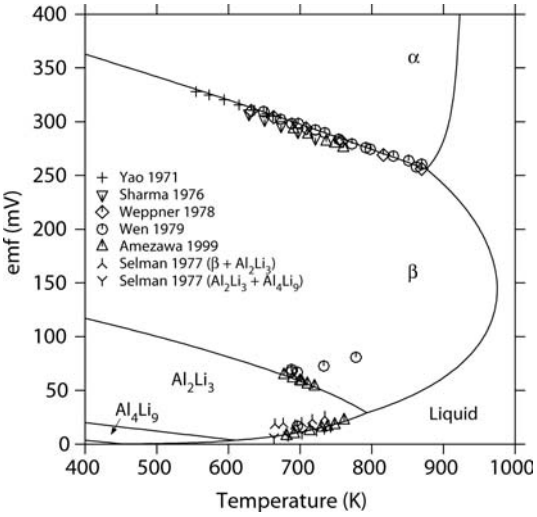

Fig. 11. Calculated potential diagram of the Al–Li system including experimental data [35, 37, 43, 49–51]. The Li potential is expressed as emf relative to pure liquid Li.

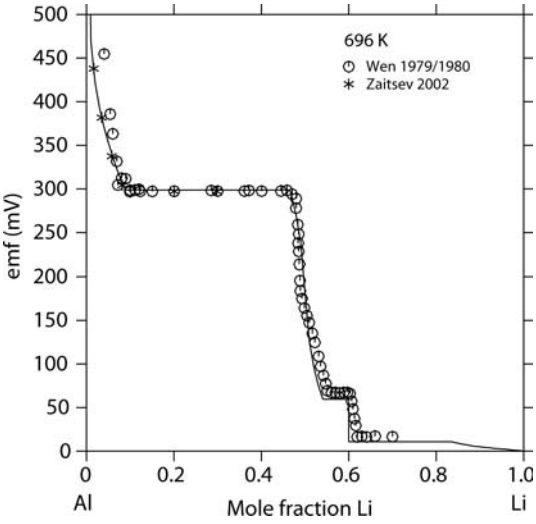

Fig. 13. Calculated Li potential at 696 K as function of Li content including experimental data [28, 35, 52]. The Li potential is expressed as emf relative to pure liquid Li.

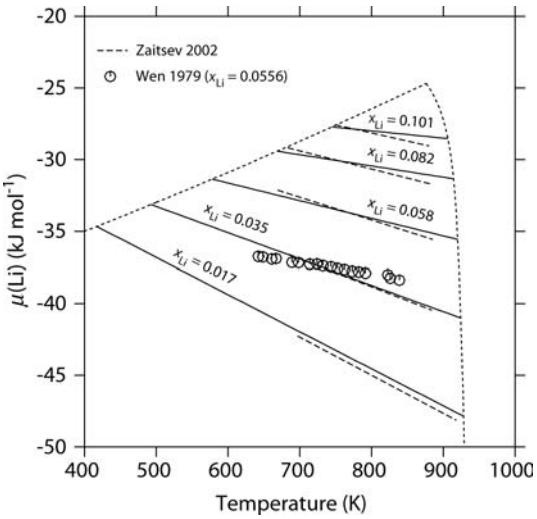

Fig. 12. Calculated Li potentials in the α single phase region at different compositions including experimental data [35, 52]. The dotted lines delineate the α single phase region. The Li potential is given relative to pure liquid Li.

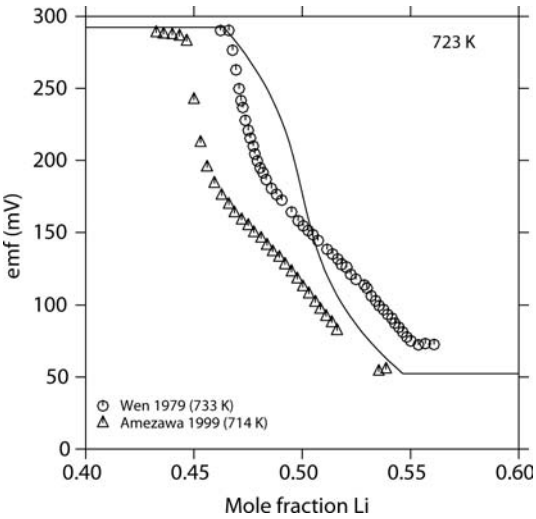

Fig. 14. Calculated Li potential at 723 K across the β phase region including experimental data [35, 37]. The Li potential is expressed as emf relative to pure liquid Li.

tal data on both the phase diagram and thermodynamic properties, the presented dataset can be considered fairly safe in the sense that Gibbs energies, enthalpies and entropies given cannot differ much from their true values. The most obvious missing piece of information concerns the Al solubility in solid Li. The ordering modelling presented cannot be considered quite mature. Here, there is probably some room for improvement.

The authors gratefully acknowledge the financial support from the Deutsche Forschungsgemeinschaft (DFG) within the Collaborative Research Centre (SFB) 289 "Forming of metals in the semi-solid state and their properties".

References

[1] E.J. Lavernia, N.J. Grant: J. Mater. Sci. 22 (1987) 1521.
[2] H.M. Flower, P.J. Gregson: Mater. Sci. Technol. 3 (1987) 81.
[3] N. Gao, M.J. Starink, L. Davin, A. Cerezo, S.C. Wang, P.J. Gregson: Mater. Sci. Technol. 21 (2005) 1010.
[4] M.S. Whittingham: Chem. Rev. 104 (2004) 4271.
[5] E.C. Gay, D.R. Vissers, F.J. Martino, K.E. Anderson: J. Electrochem. Soc. 123 (1976) 1591.
[6] M.-L. Saboungi, C.C. Hsu: CALPHAD 1 (1977) 237.
[7] A.J. McAlister: Bull. Alloy Phase Diagrams 3 (1982) 177.
[8] C. Sigli, J.M. Sanchez: Acta Metall. 34 (1986) 1021.
[9] S.-W. Chen, C.-H. Jan, J.-C. Lin, Y.A. Chang: Metall. Trans. A 20 (1989) 2247.
[10] N. Saunders: Z. Metallkd. 80 (1989) 894.
[11] W. Cao, J. Zhu, F. Zhang, W.A. Oates, M. Asta, Y.A. Chang: Acta Mater. 54 (2006) 377.
[12] P. Aßmann: Z. Metallkd. 18 (1926) 51.
[13] A. Müller: Z. Metallkd. 18 (1926) 231.
[14] G. Grube, L. Mohr, W. Breuning: Z. Elektrochem. 41 (1935) 880.
[15] F.I. Shamray, P.Y. Saldau: Izv. Akad. Nauk SSSR, Otdel. Khim. (1937) 631 (cited from [7]).
[16] K.M. Myles, F.C. Mrazek, J.A. Smaga, J.L. Settle, in: Advanced Battery Research and Design, U.S. ERDA Report ANL-76-8, Proc. Symp. and Workshop, Argonne National Laboratory (1976) B 50 (cited from [7]).
[17] K.-F. Tebbe, H.G. von Schnering, B. Rüter, G. Rabeneck: Z. Naturforsch. B 28 (1973) 600.
[18] D.A. Hansen, J.F. Smith: Acta Crystallogr. B 24 (1968) 913.
[19] E. Schürmann, H.-J. Voss: Giessereiforschung 33 (1981) 33.
[20] R.J. Pulham, P. Hubberstey, P. Hemptenmacher: J. Phase Equilib. 15 (1994) 587.
[21] H. Vosskühler: Metallwirtschaft Metallwissenschaft Metalltechnik 16 (1937) 907 (cited from [22]).
[22] S.K. Nowak: J. Met. 8 (1956) 553.
[23] W.R.D. Jones, P.P. Das: J. Inst. Met. 87 (1958) 338.
[24] L.P. Costas, R.P. Marshall: Trans. Metall. Soc. AIME 224 (1962) 970.
[25] E.D. Levine, E.J. Rapperport: Trans. Metall. Soc. AIME 227 (1963) 1204.
[26] R. Nozato, G. Nakai: Trans. Japan Inst. Met. 18 (1977) 679.
[27] E. Schürmann, I.K. Geißler: Giessereiforschung 32 (1980) 165.
[28] C.J. Wen, W. Weppner, B.A. Boukamp, R.A. Huggins: Metall. Trans. B 11 (1980) 131.
[29] B. Noble, G.E. Thompson: Met. Sci. J. 5 (1971) 114.
[30] D.B. Williams, J.W. Edington: Met. Sci. 9 (1975) 529.
[31] G. Cocco, G. Fagherazzi, L. Schiffini: J. Appl. Crystallogr. 10 (1977) 325.
[32] D.-R. Liu, D.B. Williams: Scr. Metall. 22 (1988) 1361.
[33] C.-S. Tsao, C.-Y. Chen, J.-Y. Huang: Phys. Rev. B 70 (2004) 174104.
[34] K. Kishio, J.O. Brittain: J. Phys. Chem. Solids 40 (1979) 933.
[35] C.J. Wen, B.A. Boukamp, R.A. Huggins, W. Weppner: J. Electrochem. Soc. 126 (1979) 2258.
[36] E. Veleckis: J. Less-Common Met. 73 (1980) 49.
[37] K. Amezawa, N. Yamamoto, Y. Tomii, Y. Ito: J. Electrochem. Soc. 146 (1999) 1069.
[38] N.E. Christensen: Phys. Rev. B 32 (1985) 207.
[39] X.-Q. Guo, R. Podloucky, A.J. Freeman: Phys. Rev. B 42 (1990) 10912.
[40] A. Arya, G.P. Das, H.G. Salunke, S. Banerjee: J. Phys. Condens. Matter 6 (1994) 3389.
[41] G.P. Das, A. Arya, S. Banerjee: Intermetallics 4 (1996) 625.
[42] M.H.F. Sluiter, Y. Watanabe, D. de Fontaine, Y. Kawazoe: Phys. Rev. B 53 (1996) 6137.
[43] N.P. Yao, L.A. Herédy, R.C. Saunders: J. Electrochem. Soc. 118 (1971) 1039.
[44] V.D. Bushmanov, S.P. Yatsenko: Russ. J. Phys. Chem. 55 (1981) 1680.
[45] Z. Moser, F. Sommer, B. Predel: Z. Metallkd. 79 (1988) 705.
[46] J.-J. Lee, F. Sommer: Z. Metallkd. 76 (1985) 750.
[47] J.-M. Hicter, A. Vermandé, I. Ansara, P. Desré: Rev. int. hautes Tempér. Réfract. 8 (1971) 197.
[48] S.P. Yatsenko, E.A. Saltykova: Russ. J. Phys. Chem. 48 (1974) 1402.
[49] R.A. Sharma, R.N. Seefurth: J. Electrochem. Soc. 123 (1976) 1763.
[50] J.R. Selman, D.K. DeNuccio, C.J. Sy, R.K. Steunenberg: J. Electrochem. Soc. 124 (1977) 1160.
[51] W. Weppner, R.A. Huggins: J. Electrochem. Soc. 125 (1978) 7.
[52] A.I. Zaitsev, A.D. Litvina, N.E. Zaitseva: Russ. J. Inorg. Chem. 47 (2002) 255.
[53] A.T. Dinsdale: CALPHAD 15 (1991) 317.
[54] E.A. Guggenheim: Trans. Faraday Soc. 33 (1937) 151.
[55] O. Redlich, A.T. Kister: Ind. Eng. Chem. 40 (1948) 345.
[56] W. Gorsky: Z. Phys. 50 (1928) 64.
[57] W.L. Bragg, E.J. Williams: Proc. Royal Soc. London, Ser. A 145 (1934) 699.
[58] A. Kusoffsky, N. Dupin, B. Sundman: CALPHAD 25 (2001) 549.
[59] G. Inden: Acta Metall. 22 (1974) 945.
[60] B. Hallstedt, N. Dupin, M. Hillert, L. Höglund, H.L. Lukas, J.C. Schuster, N. Solak: CALPHAD 31 (2007) 28.
[61] J.-O. Andersson, T. Helander, L. Höglund, P. Shi, B. Sundman: CALPHAD 26 (2002) 273.
[62] V.A. Vertogradskii, N.A. Parkhomenko, I.N. Bel'skaya: Russ. Metall. (1995) 138.

(Received April 10, 2007; accepted July 10, 2007)

Bibliography

DOI 10.3139/146.101553
Int. J. Mat. Res. (formerly Z. Metallkd.)
98 (2007) 10; page 961–969

ISSN 1862-5282

Correspondence address

Dr. Bengt Hallstedt
Materials Chemistry
RWTH Aachen University
Kopernikusstr. 16, D-52056 Aachen, Germany
Tel.: +49 241 802 5972
Fax: +49 241 802 2295
E-mail: hallstedt@mch.rwth-aachen.de